

The S2 Gene Nucleotide Sequences of Prototype Strains of the Three Reovirus Serotypes: Characterization of Reovirus Core Protein $\sigma 2$

TERENCE S. DERMODY,^{1,2,*} LESLIE A. SCHIFF,^{1,†} MAX L. NIBERT,^{1,3} KEVIN M. COOMBS,^{1,§}
AND BERNARD N. FIELDS^{1,2,4}

*Department of Microbiology and Molecular Genetics¹ and Shipley Institute of Medicine,⁴ Harvard Medical School, and
Departments of Medicine² and Pathology,³ Brigham & Women's Hospital, Boston, Massachusetts 02115*

Received 11 April 1991/Accepted 22 July 1991

The S2 gene nucleotide sequences of prototype strains of the three reovirus serotypes were determined to gain insight into the structure and function of the S2 translation product, virion core protein $\sigma 2$. The S2 sequences of the type 1 Lang, type 2 Jones, and type 3 Dearing strains are 1,331 nucleotides in length and contain a single large open reading frame that could encode a protein of 418 amino acids, corresponding to $\sigma 2$. The deduced $\sigma 2$ amino acid sequences of these strains are very conserved, being identical at 94% of the sequence positions. Predictions of $\sigma 2$ secondary structure and hydrophobicity suggest that the protein has a two-domain structure. A larger domain is suggested to be formed from the amino-terminal three-fourths of $\sigma 2$ sequence, which is separated from a smaller carboxy-terminal domain by a turn-rich hinge region. The carboxy-terminal domain includes sequences that are more hydrophilic than those in the rest of the protein and contains sequences which are predicted to form an α -helix. A region of striking similarity was found between amino acids 354 and 374 of $\sigma 2$ and amino acids 1008 and 1031 of the β subunit of the *Escherichia coli* DNA-dependent RNA polymerase. We suggest that the regions with similar sequence in $\sigma 2$ and the β subunit form amphipathic α -helices which may play a related role in the function of each protein. We have also performed experiments to further characterize the double-stranded RNA-binding activity of $\sigma 2$ and found that the capacity to bind double-stranded RNA is a property of the $\sigma 2$ protein of prototype strains and of the S2 mutant *tsC447*.

Virions of the mammalian reoviruses consist of a double protein shell formed by an inner core and an outer capsid. The virion core contains the 10 double-stranded RNA (dsRNA) genome segments and consists of three major proteins ($\lambda 1$, $\lambda 2$, and $\sigma 2$) and two minor proteins ($\lambda 3$ and $\mu 2$) (63). Previous studies of core structure suggest that $\lambda 1$ and $\sigma 2$ are complexed (33) and that $\sigma 2$ is located primarily on the inner surface of the core (68). Pentamers of the other major core protein $\lambda 2$ form the core spikes located at the vertices of the virion icosahedron (54). Crystals of the reovirus type 3 Dearing (T3D) core have been isolated and characterized (16); however, structural resolution at the atomic level awaits further studies.

The intact reovirus core contains all of the enzymatic activities necessary for viral RNA transcription and replication (13); however, solubilization of the core results in the loss of these activities (68). Insight into the function of individual core proteins has been possible through biochemical and genetic studies and through an analysis of their deduced amino acid sequences. The $\lambda 1$ protein has been shown to bind reovirus dsRNA and zinc in blotting assays (60), and $\lambda 1$ has a nucleotide-binding sequence and a TF IIIA-like zinc finger motif (6). The $\lambda 2$ protein is the reovirus guanylyltransferase (15), and $\lambda 2$ has a GTP-binding sequence

(62). The pH dependence of transcription is genetically associated with the $\lambda 3$ -encoding L1 gene segment (20), suggesting that the $\lambda 3$ protein is involved in reovirus RNA-dependent RNA polymerase activity. Furthermore, $\lambda 3$ has sequence similarity to the RNA-dependent RNA polymerases of several viruses, further suggesting that it is a component of the reovirus RNA polymerase (43, 44). The $\sigma 2$ protein is encoded by the S2 gene segment (42, 46), and similar to the other reovirus core proteins, the functions of $\sigma 2$ are not precisely understood. However, a temperature-sensitive (*ts*) mutant of T3D whose mutation maps to the S2 gene (*tsC447*) synthesizes approximately 5% of the wild-type level of single-stranded RNA (ssRNA) and assembles virions which contain only 0.1% of the normal amount of dsRNA when grown at the restrictive temperature (57). Furthermore, Schiff et al. (60) have shown that $\sigma 2$, like $\lambda 1$, binds reovirus dsRNA in a blotting assay. Thus, these data suggest that $\sigma 2$ may play a role in viral RNA synthesis or in virion assembly.

In order to learn more about the structure and function of $\sigma 2$, we determined the S2 gene nucleotide sequences of prototype strains of the three reovirus serotypes. We found that the deduced $\sigma 2$ amino acid sequences of the type 1 Lang (T1L), type 2 Jones (T2J), and T3D strains are of equal length and are highly conserved. Predictions of protein secondary structure, hydrophobicity, and surface probability suggest a two-domain model for the structure of $\sigma 2$. The amino-terminal three-fourths of the $\sigma 2$ sequence is suggested to form a large domain; the carboxy-terminal one-fourth of $\sigma 2$ is suggested to form a small domain which contains a region of sequence with similarity to a region in the *Escherichia coli* DNA-dependent RNA polymerase β subunit. We have also extended studies of the dsRNA-binding activity of

* Corresponding author.

† Present address: Lamb Center for Pediatric Research, Division of Pediatric Infectious Diseases, Vanderbilt University Medical Center, Nashville, TN 37232.

‡ Present address: Department of Microbiology, University of Minnesota Medical School, Minneapolis, MN 55455.

§ Present address: Department of Medical Microbiology, University of Manitoba, Winnipeg, Manitoba, Canada R3E 0W3.

$\sigma 2$ in a Northwestern (RNA blotting) assay and have found that the characteristics of $\sigma 2$ binding to dsRNA are clearly distinct from those of other reovirus dsRNA-binding proteins. This study represents an initial step in the understanding of structure-function relationships of the reovirus core protein, $\sigma 2$.

MATERIALS AND METHODS

Cells and viruses. Spinner-adapted mouse L929 (L) cells were grown in either suspension or monolayer cultures in Joklik's modified Eagle's minimal essential medium (Irvine Scientific, Santa Ana, Calif.) that was supplemented to contain 5% fetal calf serum (Hyclone Laboratories, Logan, Utah), 2 mM glutamine, 1 U of penicillin per ml, and 1 μ g of streptomycin per ml (Irving Scientific). Reovirus strains T1L, T2J, and T3D are laboratory stocks. Second- and third-passage L-cell lysate stocks of twice-plaque-purified reovirus were used to make purified virion preparations (25).

Sequencing dsRNA with primers. Genomic dsRNA was purified from virions according to the method described by Nibert et al. (49). The dsRNA sequences were determined by using dideoxy sequencing reactions with oligonucleotide primers, reverse transcriptase (Boehringer Mannheim Biochemicals, Indianapolis, Ind.), and [³⁵S]dATP (1,000 Ci/mmol; Amersham, Arlington Heights, Ill.), according to the method described by Bassel-Duby et al. (8). Oligonucleotide primers were made with an Applied Biosystems oligonucleotide synthesizer (Applied Biosystems, Foster City, Calif.) and were purified by C-18 Sep-Pak column chromatography (Waters Associates, Milford, Mass.) (3). Initial primers were synthesized corresponding to the T3D S2 gene nucleotide sequence (12), and additional primers corresponding to the T1L and T2J S2 gene nucleotide sequences were synthesized as necessary. Primers were synthesized at approximately 200-nucleotide intervals in order to determine the full-length sequence of each complementary strand.

Analysis of the S2 nucleotide and deduced $\sigma 2$ amino acid sequences. Sequence alignment was facilitated by the global alignment program GAP (19) from the University of Wisconsin Genetics Computer Group (UWGCG; Madison, Wisc.). Open reading frames in the S2 nucleotide sequences were determined by using the David Mount sequence analysis package (Genetics Software Center, Tucson, Ariz.). Determinations of deduced $\sigma 2$ protein amino acid composition, molecular weight, and isoelectric point were facilitated by the protein sequence analysis program PEP from the Intelligent Suite (Intelligenetics, Mountain View, Calif.).

Predictions of protein structure. Secondary-structure propensity values for $\sigma 2$ were assigned to each amino acid residue according to the method of Chou and Fasman (14) (α -helix, β -strand, and β -turn) and Leszczynski and Rose (40) (Ω -loop), and plots of secondary-structure predictions for $\sigma 2$ were generated by the technique of Nibert et al. (49). Secondary-structure predictions were also derived by the technique of Ralph et al. (55) as applied in the program PRSTRUC, provided by the Molecular Biology Computer Research Resource (MBCRR; Boston, Mass.), using the secondary-structure propensity values of Chou and Fasman (14) and Leszczynski and Rose (40). For each secondary-structure propensity type, the seed threshold and extension limit values defined by Ralph et al. (55) were used. This technique generated more than a single secondary-structure prediction for some positions in the $\sigma 2$ amino acid sequences. Hydropathicity index values for $\sigma 2$ were assigned to each amino acid residue according to the method of Kyte

and Doolittle (36), and hydropathicity plots were generated by a modification of the technique of Nibert et al. (49), in which the hydropathicity values of individual residues were averaged for each seven consecutive positions in the $\sigma 2$ sequence. Surface probability values for $\sigma 2$ were assigned to each amino acid residue according to the method of Emini et al. (22), and surface probability plots were generated by using the program PEPTIDESTRUCTURE from the UWGCG.

Data base searches. Searches of the National Biomedical Research Foundation (NBRF) data base were performed with the BLASTP program (1) provided by the MBCRR. Searches of the NBRF and Swiss protein data bases were also performed with the FASTA program (52) through BIONET (Mountain View, Calif.). Searches of a protein sequence pattern data base were conducted with the PLSEARCH program (64), provided by the MBCRR. Searches for protein sequences of potential biologic significance were facilitated by the PROSITE program from PCGENE (Intelligenetics).

SDS-PAGE of viral proteins. Discontinuous sodium dodecyl sulfate-polyacrylamide gel electrophoresis (SDS-PAGE) was performed as described by Laemmli (37). Gels were stained with Coomassie brilliant blue R-250 (Sigma Chemical Co., St. Louis, Mo.) and dried between cellophane. Alternatively, gels containing ³⁵S-labeled proteins were treated with Enlightening (New England Nuclear Corp., Boston, Mass.), dried under a vacuum, and exposed to XAR film (Eastman Kodak Co., Rochester, N.Y.) at -70°C .

Northwestern blotting. Proteins were electrophoretically transferred from SDS-polyacrylamide gels to nitrocellulose (Trans-Blot; Bio-Rad, Richmond, Calif.) by the Western immunoblotting technique (66) with Tris-glycine transfer buffer that contained 0.01% SDS and 20% (vol/vol) methanol. Northwestern blots (10) were performed as described by Schiff et al. (60). After the electrophoretic transfer of proteins to nitrocellulose, unreacted sites on the membrane were blocked with standard binding buffer (10 mM Tris-hydrochloride [pH 7.0], 1 mM EDTA, 50 mM NaCl, 0.04% bovine serum albumin, 0.04% Ficoll 400, 0.04% polyvinylpyrrolidone-40). The blotted proteins were probed with ³²P-labeled reovirus genomic dsRNA (1×10^4 to 5×10^4 cpm/ml) in binding buffer modified to contain 25 mM NaCl and 10 mM Tris-hydrochloride (pH 6.5). Unbound RNA was removed by briefly washing the nitrocellulose filter in modified binding buffer. Nitrocellulose filters were air-dried and exposed to XAR film (Kodak) at -70°C with an intensifying screen (Cronex Lightning-Plus; E. I. du Pont de Nemours & Co., Wilmington, Del.). The reovirus genomic dsRNA used as a probe was prepared from virions of T3D (60).

Chemical cleavage of $\sigma 2$ with formic acid. The protocol for chemical cleavage with formic acid described by Anders and Consigli (2) was used to generate peptide fragments of $\sigma 2$. Formic acid efficiently and specifically cleaves aspartate-proline linkages (39). Virion proteins were subjected to electrophoresis in a 5 to 10% polyacrylamide-SDS gel. The gel was fixed in 30% isopropanol-10% acetic acid, stained in a fixing solution containing 0.5% Coomassie brilliant blue R-250, and then destained in 16.5% methanol-5% acetic acid. Visualized protein bands were excised from the gel and dried by lyophilization. For formic acid treatment, gel slices containing $\sigma 2$ were swollen in 0.1 ml of 75% formic acid and then incubated in screw-cap vials at 37°C for 48 h. The reaction was stopped by removing the formic acid by lyophilization. Gel slices were equilibrated with $2 \times$ Laemmli gel sample buffer (37) until the bromphenol blue (Sigma) pH indicator remained blue. Cleavage products were analyzed

by electrophoresis of equilibrated gel slices in a 5 to 20% polyacrylamide-SDS gel.

RESULTS

Comparison of the S2 gene nucleotide sequences of prototype strains of the three reovirus serotypes. We determined the nucleotide sequences of the S2 genes of reovirus strains T1L, T2J, and T3D by using S2 genomic dsRNA that was purified from virions. The full-length S2 coding-strand sequences are shown in Fig. 1. The S2 sequence of each strain was found to be 1,331 nucleotides in length and to contain a single large open reading frame (ORF) that could encode a protein of 418 amino acids. When the S2 sequences of the three strains were compared, they were found to be identical at 958 of the 1,331 nucleotide positions (72% sequence identity). In pairwise comparisons, the T1L and T3D S2 nucleotide sequences were found to have greater similarity with each other (86% sequence identity) than either was found to have with the T2J S2 sequence (78% identity for each two-sequence comparison).

These results include the first S2 nucleotide sequence reported for strain T2J. The S2 sequences of strains T1L and T3D were reported previously (12, 27, 73) but differ in several instances from the sequences determined in this study. In the case of the T1L S2 sequence, our results include an additional cytosine between nucleotides 986 and 987 of the previously reported sequence (27). In the case of the T3D S2 sequence, our results confirm the sequence reported by Wiener et al. (73); both sequences include an additional cytosine between nucleotides 945 and 946 of the previously reported sequence (12). The corrections of previous T1L and T3D sequences are significant in that they add a single nucleotide to the $\sigma 2$ -encoding region of each S2 sequence and thereby permit the ORF encoding $\sigma 2$ to extend to nearer the 3' end of each S2 gene. As a consequence, the T1L, T2J, and T3D S2 genes have coding-strand sequences that contain small, identically sized 5' and 3' noncoding regions: 18 and 56 nucleotides, respectively (Table 1).

The determination of full-length S2 nucleotide sequences for prototype strains of the three reovirus serotypes has allowed us to identify several additional ORFs in the S2 genes of these strains. The largest ORF that is conserved in all three S2 sequences (other than that proposed to encode $\sigma 2$) is 102 nucleotides in length (nucleotides 1214 to 1315) and potentially encodes a protein of 34 amino acids. The resulting T1L, T2J, and T3D proteins would have 44% sequence identity, but there is no evidence to suggest that this short ORF is translated into protein in reovirus-infected cells. In fact, the S2 sequences of the three strains contain cytosines at nucleotides 1211 and 1217 (the -3 and +4 positions, respectively, with respect to the initiator AUG of the short ORF), so that this ORF is unlikely to be translated according to the rules of Kozak (35).

Comparison of the deduced $\sigma 2$ amino acid sequences of prototype strains of the three reovirus serotypes. We examined the deduced $\sigma 2$ amino acid sequences of the T1L, T2J, and T3D strains in order to identify conserved and variable features of $\sigma 2$. Protein length was found to be conserved in

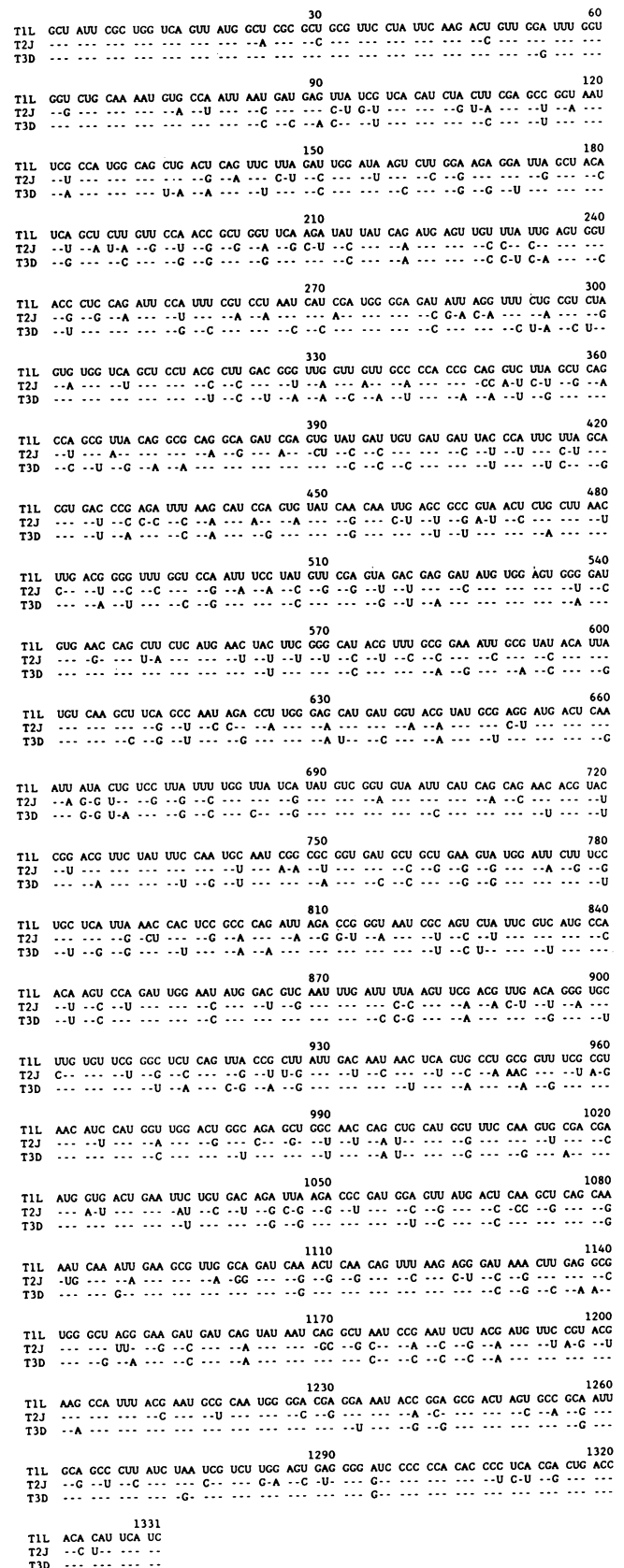


FIG. 1. Coding-strand nucleotide sequences of the reovirus T1L, T2J, and T3D S2 gene segments. Nucleotide positions are numbered above the sequences, and residues in T2J and T3D identical to those in T1L are indicated by dashes.

TABLE 1. Lengths of noncoding regions of reovirus gene segments

Gene segment (references)	Virus strain(s) ^a	Length of noncoding region (no. of bases) ^b	
		5'	3'
L1 (72)	T1L, T2J, T3D	18	32
L2 (62)	T3D	13	33
L3 (6)	T3D	13	181
M1 (69)	T3D	13	80
M2 (32, 65, 71)	T1L, T2J, T3D	29	47
M3 (69)	T3D	18	57
S1 (7, 11, 21, 45, 47, 49)	T1L	13	34
	T2J	13	38
	T3D	12	36
S2 (12, 27, 73; this study)	T1L, T2J, T3D	18	56
S3 (26, 58, 70)	T1L, T2J, T3D	27	70
S4 (4, 28)	T1L, T3D	32	66

^a Reovirus strains whose indicated gene segment nucleotide sequence has been determined.

^b Determined from referenced gene segment nucleotide sequences; the termination codon in each gene segment is not considered part of the 3' noncoding region.

the strains (418 amino acids), and no gaps were needed to align the sequences (Fig. 2). The deduced σ_2 amino acid sequences of the three strains are very conserved, being identical at 393 of the 418 amino acid positions (94% sequence identity). As was the case for the S2 nucleotide sequences, the deduced T1L and T3D σ_2 sequences have greater similarity with each other (99% sequence identity) than either sequence has with T2J σ_2 (94% sequence identity for each two-sequence comparison). The most variable region in the σ_2 sequences exhibits 88% sequence identity in the three strains and is located in the carboxy-terminal one-fourth of the protein (amino acids 311 to 418). The σ_2 protein of each strain contains eight cysteine residues, which are entirely conserved in the σ_2 sequences (Fig. 2). Proline residues account for 20 to 21 amino acids and aromatic residues account for 45 to 46 amino acids in each σ_2 sequence. There are a large number of charged residues in each σ_2 sequence, a cluster of which are located in the carboxy-terminal one-fourth of the protein (amino acids 333 to 380) (Fig. 2). Of the charged residues, basic amino acids predominate in the σ_2 sequences, so that each σ_2 protein has a calculated isoelectric point of 8.33. This value approximates the isoelectric point of 7.9 reported previously for the type 3 Abney σ_2 protein (23). The molecular masses of the three σ_2 proteins calculated from the deduced σ_2 sequences are as follows: T1L, 47,130 Da; T2J, 47,065 Da; and T3D, 47,181 Da. These masses are within the range of M_r s (45,500 to 53,500) previously determined for σ_2 by SDS-PAGE (9, 56, 59).

Computer-based predictions of σ_2 structure. We used a number of computer-based techniques to gain insight into the structure of σ_2 . Because the σ_2 sequences of T1L, T2J,

and T3D are so similar, analyses carried out with each of the individual sequences exhibited only minor variations from those of the others (data not shown). A hydropathicity plot derived for T3D σ_2 by using the hydropathicity index values of Kyte and Doolittle (36) is shown in Fig. 3. This analysis was notable for a region near the carboxy terminus of σ_2 (amino acids 340 to 410) that is more consistently hydrophilic than the remainder of the protein. In contrast, the amino-terminal three-fourths of σ_2 is characterized by nonregular fluctuations between regions of moderate to high hydropathicity and hydrophilicity. The unique nature of the carboxy-terminal one-fourth of σ_2 was also demonstrated in a surface probability plot derived for T3D σ_2 by using the technique of Emini et al. (22) (Fig. 3). This technique is useful for determining more specifically whether a given amino acid in a protein sequence is likely to be exposed on the protein surface. Amino acids 340 to 410 in σ_2 have more consistently high probabilities of occurring on the protein surface than residues in the remainder of the protein. The amino-terminal three-fourths of σ_2 is characterized by small regions of moderate to high surface probability that are separated by regions of low surface probability.

We next made predictions of σ_2 secondary structure by using the technique of Nibert et al. (49). Plots of α -helix, β -strand, and β -turn scores for T3D σ_2 are shown in Fig. 4. In these analyses, a carboxy-terminal region of σ_2 also appears to be distinct from the remainder of the protein. Amino acids 330 to 380 in σ_2 are characterized by consistently high α -helix scores. This region is bounded on either side by a region with high β -turn scores (amino acids 300 to 330 and 380 to 410). In addition, β -strand scores throughout this region (amino acids 300 to 418) are low except for a region between amino acids 330 and 340. A small region at the extreme carboxy terminus of σ_2 also has high α -helix scores. In contrast to this carboxy-terminal region, the amino-terminal three-fourths of σ_2 are characterized by alternations between regions of high β -strand and high β -turn scores. Several small regions of high α -helix scores are also found in this region, including one at the extreme amino terminus of the protein. In an alternative approach to investigating σ_2 secondary structure, we used the technique described by Ralph et al. (55). The results for T3D σ_2 are shown in Fig. 2 and are in general agreement with those obtained from the plots of σ_2 secondary structure (Fig. 4). The σ_2 protein appears to include a carboxy-terminal region that is formed from α -helices and β -turns and a larger amino-terminal region that is formed predominantly from β -strands and β -turns.

Sequences in the reovirus σ_2 protein and the β subunit of bacterial RNA polymerase are similar. To learn more about σ_2 structure and function, we used several techniques to search for proteins with sequence similarity to the deduced T1L, T2J, and T3D σ_2 amino acid sequences. Using the BLASTP algorithm (1), we identified a region in each of the σ_2 sequences that has similarity with a region in the β subunit of the *E. coli* DNA-dependent RNA polymerase (50). The σ_2 region with sequence similarity to the RNA polymerase β subunit corresponds to amino acids 354 to 374 and is shown for T1L σ_2 in Fig. 5A. The regions of similar sequence in σ_2 and the β subunit include a large number of the acid and amide amino acid residues and are predicted to assume an α -helical conformation according to secondary-structure algorithms (Fig. 2 and 4) (29). When we arranged these sequences on a helical wheel projection (61), it was evident that these α -helices in the two proteins would be amphipathic, with apolar residues occupying a narrow strip

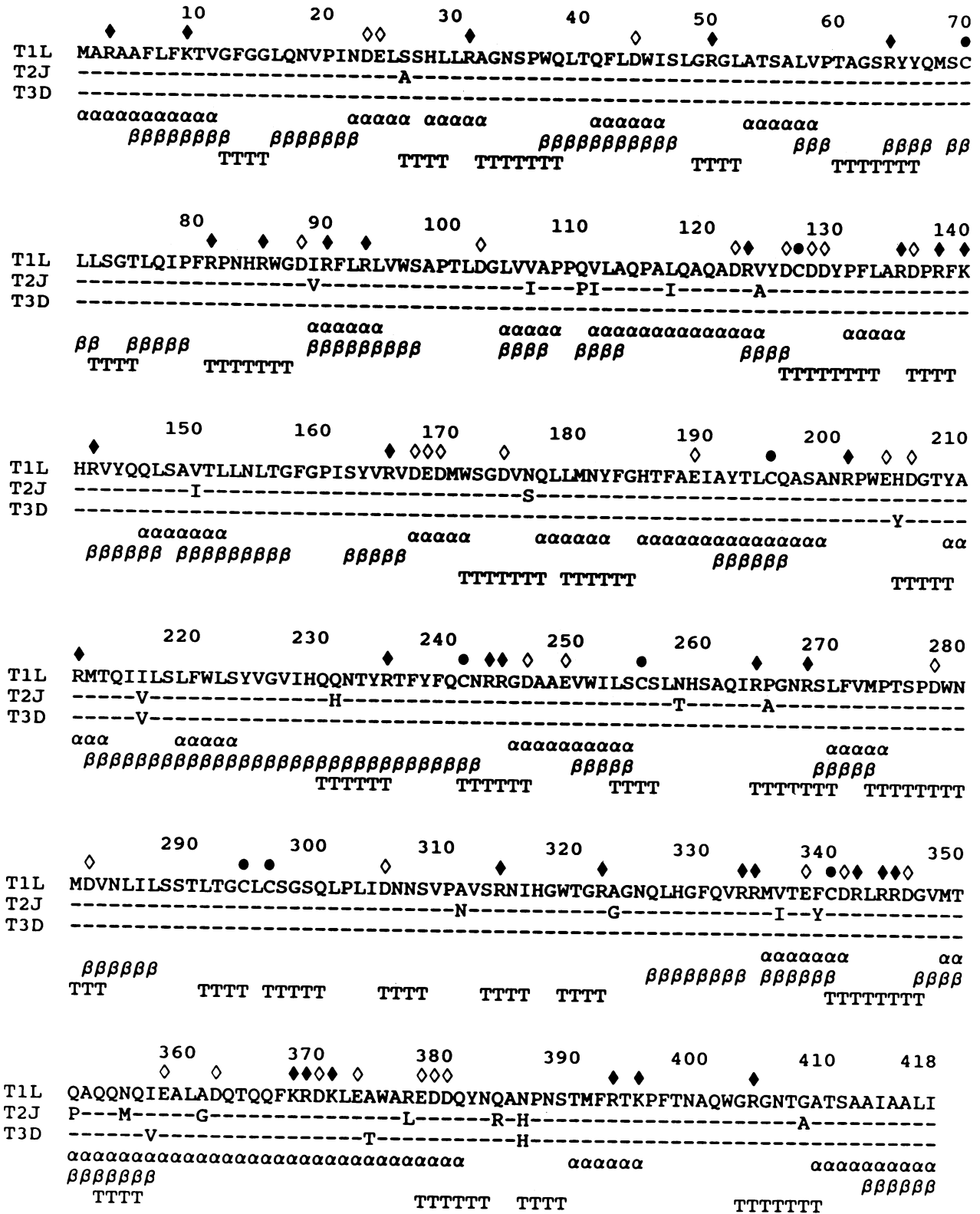


FIG. 2. Alignment of the deduced sigma 2 amino acid sequences of T1L, T2J, and T3D. The single-letter amino acid code is used. Amino acid positions are numbered above the sequences, and residues in T2J and T3D identical to those in T1L are indicated by dashes. Symbols: ●, positions of conserved cysteine residues; ◇, positions of conserved acidic residues (D, E); ◆, positions of conserved basic residues (K, R). Secondary-structure predictions (14) for T3D sigma 2 were determined by the technique of Ralph et al. (55) and are indicated for the appropriate amino acid position in the sigma 2 sequence (alpha, alpha-helix; beta, beta-strand; T, beta-turn).

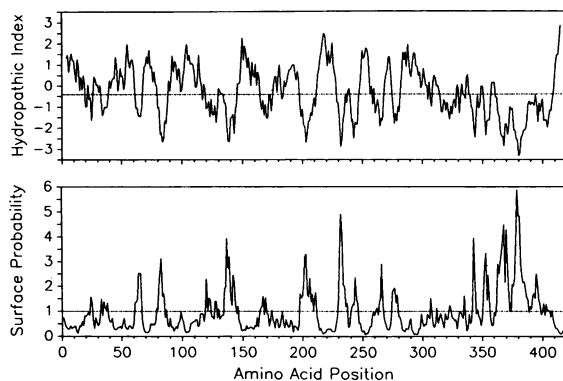


FIG. 3. Hydrophobicity and surface probability plots for T3D $\sigma 2$. Hydrophobicity values (36) for T3D $\sigma 2$ were plotted by the technique of Nibert et al. (49). The mean hydrophobicity value (-0.4) is marked with a horizontal line. Surface probability values (22) for T3D $\sigma 2$ were plotted by using the PEPTIDESTRUCTURE program from the UWGCG. The mean surface probability value (1.0) is marked with a horizontal line.

on one side of each α -helix and polar residues occupying most of the positions on the other side (Fig. 5B). The large polar side of each amphipathic α -helix would be formed almost entirely from the numerous acid and amide residues found within each sequence. These findings suggest that these α -helices in $\sigma 2$ and the β subunit of the *E. coli* DNA-dependent RNA polymerase may have related functions.

Characterization of the dsRNA-binding activity of $\sigma 2$. Although the functions of $\sigma 2$ are largely unknown, a *ts* mutant whose mutation maps to the S2 gene (*tsC447*) synthesizes 5% of the normal amount of ssRNA and assembles particles with 0.1% of the normal dsRNA content when grown at the restrictive temperature (57). In addition, $\sigma 2$ binds reovirus dsRNA in a blotting assay (60). These observations suggest that native $\sigma 2$ may also be capable of binding dsRNA and may play a role in viral RNA synthesis or in packaging the viral genome segments during virion assembly.

In order to gain further insight into the dsRNA-binding activity of $\sigma 2$, we used the Northwestern blotting technique

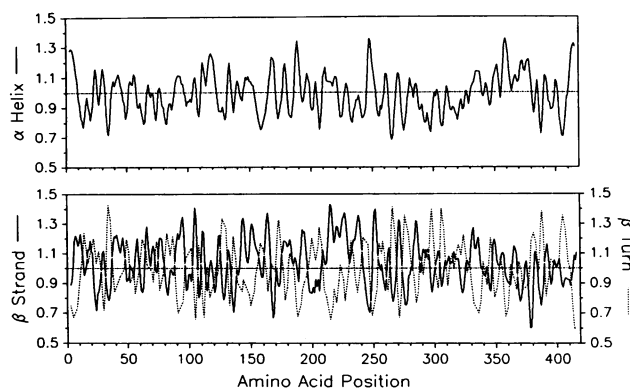


FIG. 4. Secondary-structure plots for T3D $\sigma 2$. Secondary-structure propensity scores (α -helix, β -strand, or β -turn) (14) were plotted by the technique of Nibert et al. (49). The neutral preference value for secondary structures (1.0) is marked with a horizontal line.

A

T1L $\sigma 2$ aa 354-374	Q N Q I E A L A D Q T Q Q F K R D - - - K L E A
	* * * * : * * * : * : : * * : * * * * *
RNA pol β aa 1008-1031	Q N Q L E Q L A E Q Y D E L K H E F E K K L E A

B

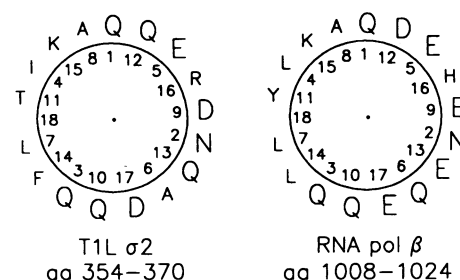


FIG. 5. (A) Region of similarity between the reovirus T1L $\sigma 2$ protein and the *E. coli* DNA-dependent RNA polymerase β subunit (RNA pol β). Symbols: *, identical amino acid (aa) residues; :, closely related residues (17). (B) Helical wheel projection (61) of a portion of the $\sigma 2$ -RNA polymerase β subunit sequence similarity. Acid (D, E) and amide (N, Q) residues are shown in larger letters than the other residues.

(10, 60) to analyze $\sigma 2$ from virions of the T1L, T2J, and T3D strains. In this assay, viral proteins were separated by SDS-PAGE, electrophoretically transferred to nitrocellulose, and probed with [$5'$ - 32 P]pCp-labeled reovirus genomic RNA. The results of the Northwestern blot shown in Fig. 6A indicate that dsRNA binding is a property of the $\sigma 2$ proteins of all three prototype strains. In order to define the conditions for optimal detection of the binding of $\sigma 2$ to dsRNA, we determined the effects of varying the pH and NaCl concentration on the dsRNA-binding activity of T3D $\sigma 2$. The $\sigma 2$ dsRNA-binding activity could be detected at pH 5.5 and 6.0, but was never detected at a pH greater than 6.5 (Fig. 6B). Furthermore, the dsRNA-binding activity of $\sigma 2$ was detected only in binding buffers with NaCl concentrations of ≤ 50 mM (data not shown). These characteristics are clearly distinct from those of the other reovirus dsRNA-binding proteins $\sigma 3$ and $\lambda 1$ (Fig. 6B and data not shown).

We recognized that the pH and NaCl dependence of dsRNA binding by $\sigma 2$ might enhance our ability to identify differences in this activity between reovirus strains; such differences might allow us to identify a specific region of $\sigma 2$ involved in dsRNA binding. The deduced $\sigma 2$ amino acid sequence of *tsC447*, carrying a *ts* mutation mapped to the S2 gene, was found to contain only three amino acid differences (valine 188, valine 323, and aspartate 383) from that of the T3D strain from which it was derived (73). We investigated whether the $\sigma 2$ dsRNA-binding activity of *tsC447* differed from that of T3D $\sigma 2$. In experiments in which either the pH (Fig. 6B) or the NaCl concentration (data not shown) of the binding buffer was varied, we found that there was no difference in the dsRNA-binding activity of $\sigma 2$ between the mutant and wild-type strains. In subsequent experiments with T1L and T3D, strains with differences at five amino acid positions in $\sigma 2$, we were also unable to detect any difference in the $\sigma 2$ dsRNA binding by varying either the pH or NaCl

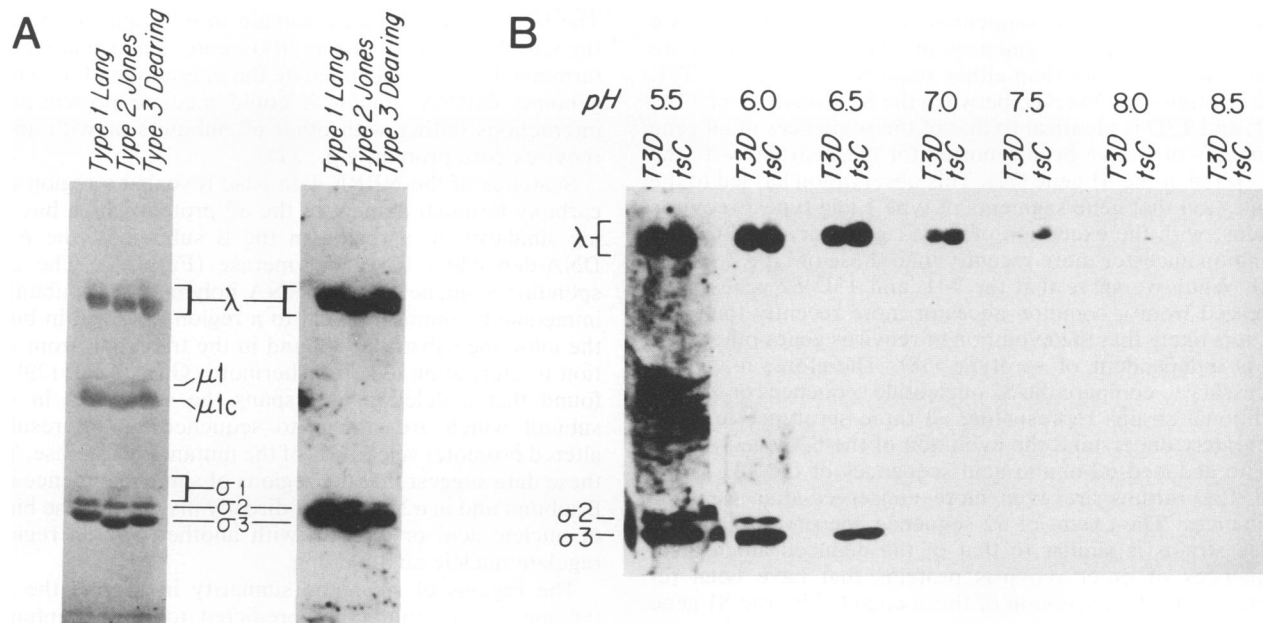


FIG. 6. (A) Binding of reovirus proteins to reovirus genomic RNA. Viral proteins from 5×10^{11} purified reovirus T1L, T2J, and T3D were separated on a 5 to 10% polyacrylamide-SDS gradient gel and electrophoretically transferred to nitrocellulose filters. The filter shown on the left was stained with amido black immediately after electrophoretic transfer. The filter shown on the right was probed with 5×10^4 cpm of $[5'-^{32}P]pCp$ -labeled reovirus genomic RNA per ml in binding buffer that had been adjusted to pH 6.0 and 25 mM NaCl after initial protein-binding sites were blocked. The filter probed with dsRNA was washed briefly in binding buffer and exposed to XAR film (Kodak) for 24 h at -70°C with an intensifying screen. Reovirus proteins are indicated between the filters. (B) Analysis of the dsRNA binding of T3D and tsC447. Viral proteins from 5×10^{11} purified reovirus T3D and tsC447 virions were separated on a 5 to 20% polyacrylamide-SDS gradient gel and electrophoretically transferred to a nitrocellulose filter. Protein-binding sites were blocked in standard binding buffer, and the filter was cut so that pairs of lanes could be probed with 5×10^4 cpm of $[5'-^{32}P]pCp$ -labeled reovirus genomic RNA per ml in binding buffer that had been adjusted to the indicated pH. The filters were washed briefly in binding buffer and exposed to XAR film (Kodak) for 24 h at -70°C with an intensifying screen. Reovirus proteins are indicated on the left.

concentration (data not shown). Thus, using this approach, we could not implicate any of the residues in $\sigma 2$ that differ between these reovirus strains in the dsRNA-binding activity of the $\sigma 2$ protein.

We also performed Northwestern blotting studies of $\sigma 2$ peptide fragments generated by chemical cleavage with 75% formic acid. Treatment with formic acid has been used to cleave proteins specifically between aspartate and proline residues (39). In the case of $\sigma 2$, formic acid treatment resulted in the generation of two fragments with M_r s of 17,000 and 29,000 (data not shown), consistent with the presence of a single aspartate-proline pair (amino acids 136 and 137) in the deduced amino acid sequence of $\sigma 2$. In experiments that used amounts of $\sigma 2$ that permit the detection of the dsRNA-binding activity of intact $\sigma 2$, we were unable to detect dsRNA binding by either fragment (data not shown).

DISCUSSION

Reovirus gene segments have short 5' and 3' noncoding sequences. In this study, we determined the S2 gene nucleotide sequences of prototype strains of the three reovirus serotypes. The S2 sequences of reovirus strains T1L and T2J in this report and of strain T3D in this and a previous report (73) have short 5' and 3' noncoding sequences (18 and 56 nucleotides, respectively). These S2 gene sequences differ from previously published S2 sequences (12, 27) that identified longer 3' noncoding regions. In the S2 sequences deter-

mined for each of the prototype strains in this study, the long ORF in S2 proposed to encode the $\sigma 2$ protein is 418 amino acids in length. The molecular mass of $\sigma 2$ calculated from these deduced amino acid sequences of T1L, T2J, and T3D (~47 kDa) is consistent with the M_r s of $\sigma 2$ determined in previous studies (9, 56, 59).

Having short 5' and 3' noncoding sequences is a quality that appears to be common to all gene segments of the mammalian reoviruses, including S2. Reovirus gene segments for which nucleotide sequences have been reported to date have 5' noncoding regions of 32 nucleotides (S4) or less and 3' noncoding regions of 181 nucleotides (L3) or less (Table 1). It has been observed that the addition of a single base near the 3'-terminal end of the published L3 nucleotide sequence (6) would result in a $\lambda 1$ ORF with a 3' noncoding region of only 35 nucleotides (48); therefore, it is possible that the published L3 sequence contains an error near its 3' end and that the longest 3' noncoding region in the reovirus genome is 80 nucleotides (M1). The economy exhibited in the size of the noncoding sequences of the mammalian reoviruses also appears to be common among other viruses containing segmented genomes, including simian rotavirus (43), bluetongue virus (24), and influenza virus (38). Thus, the replication strategies of members of the *Reoviridae* and the *Orthomyxoviridae* must permit noncoding sequences to constitute a minimal part of their genomes.

Comparison of the S2 nucleotide and $\sigma 2$ amino acid sequences of prototype strains of the three reovirus serotypes.

The S2 gene nucleotide sequences of T1L, T2J, and T3D are very similar, and the sequences of T1L and T3D are more similar to each other than either sequence is to that of T2J. The relationship observed between the S2 sequences of T1L, T2J, and T3D is identical to that of the sequences of all gene segments that have been reported for these strains with the exception of the S1 gene (72). This observation has led to the suggestion that gene segments of type 1 and type 3 reovirus strains, with the exception of the S1 gene, diverged from a common ancestor more recently than those of type 2 strains (72). While we agree that the T1L and T3D S2 genes have diverged from a common ancestor more recently than T2J S2, it is likely that the evolution of reovirus genes other than S1 is independent of serotype (18). Therefore, it will be necessary to compare the S2 nucleotide sequences of several additional strains representing all three serotypes to more accurately understand the evolution of the S2 gene.

The deduced $\sigma 2$ amino acid sequences of the T1L, T2J, and T3D strains are even more conserved than their S2 sequences. The extent of $\sigma 2$ sequence conservation among these strains is similar to that of the deduced amino acid sequences of other reovirus proteins that have been reported, with the exception of those encoded by the S1 gene (72). This extent of amino acid sequence conservation may be due to evolutionary constraints placed on either the structure or function of reovirus proteins other than the S1 gene products, $\sigma 1$ and $\sigma 1s$. Alternatively, there may be unique selection pressures (e.g., immune) operating on the S1 gene products, resulting in the observed sequence heterogeneity of the $\sigma 1$ and $\sigma 1s$ proteins.

Two-domain model for the structure of $\sigma 2$. An analysis of computer-based predictions of $\sigma 2$ structure (Fig. 2 through 4) suggests that the $\sigma 2$ protein contains two distinct regions which form independent domains. In particular, the carboxy-terminal one-fourth of the $\sigma 2$ sequence is characterized by large hydrophilic regions, which correspond to sequences predicted to form α -helix and β -turn structures. Furthermore, a large number of residues in this region of $\sigma 2$ are likely to be exposed on the protein surface. In contrast, the amino-terminal three-fourths of the $\sigma 2$ sequence is characterized by large hydrophobic regions, and predictions of protein secondary structure suggest that this region of $\sigma 2$ is formed predominantly from β -strands which alternate with β -turns. The appearance of regions of low surface probability separated by regions of high surface probability in this region of $\sigma 2$ also suggests that it is formed predominantly from alternating β -strands and β -turns. The amino-terminal and carboxy-terminal domains appear to be separated by sequences with strong β -turn (Fig. 2 and 4) and Ω -loop (data not shown) predictions, and this region may form a hinge between the two domains.

The multidomain structural model that we propose for $\sigma 2$, a major core protein of reovirus, is reminiscent of the structures of the capsid proteins of several other small RNA-containing viruses that have been determined by X-ray crystallography (31). Recently, the same multidomain structural motif has been observed in a small isometric DNA-containing virus (67). The multiple domains of several of these small isometric virus capsid proteins perform different functions; a small (usually amino-terminal) basic domain interacts with the viral genome, and other domains are involved in the protein-protein interactions that generate the virus capsid shell. The proposed structural similarity between $\sigma 2$ and the capsid proteins of these other viruses suggests that, like these other virus capsid proteins, the different domains in $\sigma 2$ might also have different functions.

The large amino-terminal domain in $\sigma 2$ might form part of the icosahedral shell of the virion core. The small carboxy-terminal domain could mediate the interaction of $\sigma 2$ with the genomic dsRNA, and/or it could mediate protein-protein interactions (either with other $\sigma 2$ subunits or with another reovirus core protein, e.g., $\lambda 1$).

Searches of the NBRF data base revealed a region in the carboxy-terminal domain of the $\sigma 2$ protein which has striking similarity to a region in the β subunit of the *E. coli* DNA-dependent RNA polymerase (Fig. 5A). The corresponding sequences in the RNA polymerase β subunit are immediately amino-terminal to a region involved in binding the initiating substrate (30) and in the transition from initiation to elongation (34). Furthermore, Glass et al. (29) have found that a deletion that spans the sequences in the β subunit which are similar to sequences in $\sigma 2$ results in altered promoter selectivity of the mutant polymerase. Thus, these data suggest that the regions of similar sequence in the β subunit and in $\sigma 2$ are either directly involved in the binding of nucleic acid or interact with another protein region to regulate nucleic acid binding.

The regions of sequence similarity in $\sigma 2$ and the RNA polymerase β subunit are predicted to form amphipathic α -helices which include a number of acidic residues and would be expected to have a net negative charge (Fig. 5B). The $\sigma 2$ sequence with similarity to the β subunit is within the region predicted to form the largest α -helix in $\sigma 2$ (amino acids 348 to 381). This large α -helical region has a net charge of -3 in T1L and T3D $\sigma 2$ and -4 in T2J $\sigma 2$; therefore, it is unlikely that it is directly involved in the binding of nucleic acid (5, 51). Negatively charged amphipathic α -helices have been implicated as playing key roles in proteins capable of transcriptional activation through the interaction of the α -helical regions with other proteins (53). Therefore, the acidic amphipathic α -helix in the carboxy-terminal domain of $\sigma 2$ may be involved in protein-protein interactions involving another reovirus protein(s).

The $\sigma 2$ protein binds dsRNA. In this study, we extended the findings of Schiff et al. (60) and showed that the $\sigma 2$ proteins of prototype strains of the three reovirus serotypes can bind reovirus genomic RNA in a Northwestern blotting assay. The $\sigma 2$ proteins of strains T1L, T2J, and T3D appear to bind dsRNA with similar affinity, and these proteins bind genomic RNA weakly in comparison to the other reovirus dsRNA-binding proteins, $\sigma 3$ and $\lambda 1$. While the probe used to study the dsRNA-binding activity of $\sigma 2$ (reovirus genomic RNA) would have allowed us to detect sequence-specific nucleic acid-binding activities, our experiments do not directly address the specificity of $\sigma 2$ -dsRNA binding. In fact, our experiments suggest that $\sigma 2$ binding to dsRNA is not likely to be sequence specific. The conditions which allow detection of $\sigma 2$ binding to dsRNA in this assay (pH 5.5 to 6.0; 0 to 50 mM NaCl) are very similar to those described for the RNA binding of rotavirus VP2 (10) and the DNA binding of bovine papillomavirus E2 protein (41), both of which have been characterized as sequence-independent interactions. We found that the $\sigma 2$ -dsRNA binding of *tsC447* was indistinguishable from that of T3D. Although the phenotype of *tsC447* suggests that the mutant $\sigma 2$ protein might have an altered capacity to bind genomic dsRNA, we could not demonstrate a difference between the activities of the wild-type and mutant $\sigma 2$ proteins by using the Northwestern blotting assay. This suggests that the lesion(s) in *tsC447* responsible for its phenotype does not directly affect the dsRNA-binding activity of the mutant protein and may

reflect altered interactions between mutant $\sigma 2$ and other proteins within the reovirus core.

We were unable to localize the dsRNA-binding activity of $\sigma 2$ to a particular region of the protein in experiments done with $\sigma 2$ peptide fragments generated by chemical cleavage with formic acid. This may have been due to the relatively weak dsRNA-binding activity of $\sigma 2$ observed in Northwestern blots, the modification of specific residues in $\sigma 2$ by treatment with formic acid, or the possibility that the binding of $\sigma 2$ to dsRNA may require sequences in each of the $\sigma 2$ fragments generated by cleavage with formic acid. If the dsRNA-binding activity of $\sigma 2$ requires sequences in each of these fragments, this would suggest that $\sigma 2$ -dsRNA binding resides in the large amino-terminal domain of $\sigma 2$ proposed to form part of the shell of the reovirus core.

Understanding the reovirus core. This study represents an initial step in the characterization of the $\sigma 2$ protein and is part of a continuing analysis of the reovirus core. The intact core plays an important role in packaging the reovirus genome and also mediates several distinct enzymatic activities during reovirus replication. The deduced amino acid sequences of $\sigma 2$ reported here will be essential for the interpretation of X-ray crystallographic data obtained from studies of the reovirus core currently in progress in our laboratory (16). However, given the complexity of the core particle, it will be necessary to pursue other types of studies, such as cryoelectron microscopy with image reconstruction, in order to gain insight into core structure. In addition, biochemical studies of core proteins and analyses of their amino acid sequences will allow us to learn more about the structure and function of individual core proteins. Our study will serve as a framework for future investigations concerning the role that $\sigma 2$ plays in formation of the inner shell of the core, the binding of $\sigma 2$ to reovirus dsRNA, and possible regulatory functions of $\sigma 2$ with respect to the functions of the intact core in reovirus transcription and replication.

ACKNOWLEDGMENTS

We express our appreciation to Elaine Freimont and Richard van den Broek for expert technical assistance and to Marcia Kazmierczak for help with preparing the manuscript. We are grateful to Susan Russo and Randy Smith of the MBCRR for assistance with algorithms to predict protein secondary structure and searches of protein sequence data bases and to Roger Chalkley for discussions of nucleic acid-binding proteins. We also thank Lynda Morrison and Kenneth Tyler for reviews of the manuscript.

This work was supported by research grant 5R37 1A113178 from the National Institute of Allergy and Infectious Diseases. Support to B.N.F. was also provided by the Shipley Institute of Medicine. K.M.C. was supported by training grant 5T32-AI07061 from the National Institute of Allergy and Infectious Diseases; M.L.N. was supported by Public Health Service Award 5T32 GM07753 from the National Institute of General Medical Sciences; L.A.S. was supported by Public Health Service Award 1F32 GM12478 from the National Institute of General Medicine; and T.S.D. was the recipient of Physician-Scientist Award 5K11 AI00865 from the National Institute of Allergy and Infectious Diseases.

REFERENCES

- Altschul, S. F., W. Gish, W. Miller, E. W. Myers, and D. J. Lipman. 1990. Basic local alignment search tool. *J. Mol. Biol.* **215**:403-410.
- Anders, D. G., and R. A. Consigli. 1983. Chemical cleavage of polyomavirus major structural protein VP1: identification of cleavage products and evidence that the receptor moiety resides in the carboxy-terminal region. *J. Virol.* **48**:197-205.
- Applied Biosystems. 1984. User bulletin. **13**:1-28.
- Atwater, J. A., S. M. Munemitsu, and C. E. Samuel. 1986. Biosynthesis of reovirus-specified polypeptides: molecular cDNA cloning and nucleotide sequence of the reovirus serotype 1 Lang strain S4 mRNA which encodes the major capsid surface polypeptide $\sigma 3$. *Biochem. Biophys. Res. Commun.* **136**:183-192.
- Bandziulis, R. J., M. S. Swanson, and G. Dreyfuss. 1989. RNA-binding proteins as developmental regulators. *Genes Dev.* **3**:431-437.
- Bartlett, J. A., and W. K. Joklik. 1988. The sequence of the reovirus serotype 3 L3 genome segment which encodes the major core protein $\lambda 1$. *Virology* **167**:31-37.
- Bassel-Duby, R., A. Jayasuriya, D. Chatterjee, N. Sonenberg, J. V. Maizel, Jr., and B. N. Fields. 1985. Sequence of reovirus hemagglutinin predicts a coiled-coil structure. *Nature (London)* **315**:421-423.
- Bassel-Duby, R., D. R. Spriggs, K. L. Tyler, and B. N. Fields. 1986. Identification of attenuating mutations on the reovirus type 3 S1 double-stranded RNA segment with a rapid sequencing technique. *J. Virol.* **60**:64-67.
- Both, G. W., S. Lavi, and A. J. Shatkin. 1975. Synthesis of all the gene products of the reovirus genome *in vivo* and *in vitro*. *Cell* **4**:173-180.
- Boyle, J. F., and K. V. Holmes. 1986. RNA-binding proteins of bovine rotavirus. *J. Virol.* **58**:561-568.
- Cashdollar, L. W., R. A. Chmelo, J. R. Wiener, and W. K. Joklik. 1985. The sequence of the S1 genes of the three serotypes of reovirus. *Proc. Natl. Acad. Sci. USA* **82**:24-28.
- Cashdollar, L. W., J. Esperza, G. R. Hudson, R. Chmelo, P. W. K. Lee, and W. K. Joklik. 1982. Cloning of the double-stranded RNA genes of reovirus: sequence of the cloned S2 gene. *Proc. Natl. Acad. Sci. USA* **79**:7644-7648.
- Chang, C.-T., and H. J. Zweerink. 1971. Fate of parental reovirus in infected cell. *Virology* **46**:544-555.
- Chou, P. Y., and G. D. Fasman. 1978. Empirical predictions of protein conformation. *Annu. Rev. Biochem.* **47**:251-276.
- Cleveland, D. R., H. Zarbl, and S. Millward. 1986. Reovirus guanylyltransferase is L2 gene product lambda 2. *J. Virol.* **60**:307-311.
- Coombs, K. M., B. N. Fields, and S. C. Harrison. 1990. Crystallization of the reovirus type 3 Dearing core. Crystal packing is determined by the $\lambda 2$ protein. *J. Mol. Biol.* **215**:1-5.
- Dayhoff, M. O., W. C. Barker, and L. T. Hunt. 1983. Establishing homologies in protein sequences. *Methods Enzymol.* **91**:524-545.
- Dermody, T. S., M. L. Nibert, R. Bassel-Duby, and B. N. Fields. 1990. Sequence diversity in S1 genes and S1 translation products of eleven type 3 reovirus strains. *J. Virol.* **64**:4842-4850.
- Devereux, J., P. Haeblerli, and O. Smithies. 1984. A comprehensive set of sequence analysis programs for the VAX. *Nucleic Acids Res.* **12**:387-395.
- Drayna, D., and B. N. Fields. 1982. Activation and characterization of the reovirus transcriptase: genetic analysis. *J. Virol.* **41**:110-118.
- Duncan, R., D. Horne, L. W. Cashdollar, W. K. Joklik, and P. W. K. Lee. 1990. Identification of conserved domains in the cell attachment proteins of the three serotypes of reovirus. *Virology* **174**:339-409.
- Emini, E. A., J. V. Hughs, D. S. Perlow, and J. Boger. 1985. Induction of hepatitis A virus-neutralizing antibody by a virus-specific synthetic peptide. *J. Virol.* **55**:836-839.
- Ewing, D. D., M. D. Sargent, and J. Borsa. 1985. Switch-on transcriptase function in reovirus: analysis of polypeptide changes using 2-D gels. *Virology* **144**:442-456.
- Fukusho, Y., S. Yu, and P. Roy. 1989. Completion of the sequence of bluetongue virus serotype 10 by the characterization of a structural protein, VP6, and a nonstructural protein, NS2. *J. Gen. Virol.* **70**:1677-1689.
- Furlong, D. B., M. L. Nibert, and B. N. Fields. 1988. Sigma 1 protein of mammalian reoviruses extends from the surfaces of viral particles. *J. Virol.* **62**:246-256.
- George, C. X., J. A. Atwater, and C. E. Samuel. 1986. Biosynthesis of reovirus-specified polypeptides: molecular cDNA cloning and nucleotide sequence of the reovirus serotype 1 Lang

- strain S3 mRNA which encodes the nonstructural RNA-binding protein σ NS. *Biochem. Biophys. Res. Commun.* **139**:845–851.
27. George, C. X., A. Crowe, S. M. Munemitsu, J. A. Atwater, and C. E. Samuel. 1987. Biosynthesis of reovirus-specified polypeptides: molecular cDNA cloning and nucleotide sequence of the reovirus serotype 1 Lang strain S2 mRNA which encodes the virion core polypeptide σ 2. *Biochem. Biophys. Res. Commun.* **147**:1153–1161.
 28. Giantini, M., L. S. Seliger, Y. Furuichi, and A. J. Shatkin. 1984. Reovirus type 3 genome segment S4: nucleotide sequence of the gene encoding a major virion surface protein. *J. Virol.* **52**:984–987.
 29. Glass, R. E., S. T. Jones, V. Nene, T. Nomura, N. Fujita, and A. Ishihama. 1986. Genetic studies on the β subunit of *Escherichia coli* RNA polymerase. VIII. Localisation of a region involved in promoter selectivity. *Mol. Gen. Genet.* **203**:487–491.
 30. Grachev, M. A., E. A. Lukhtanov, A. A. Mustaev, E. F. Zaychikov, M. N. Abdukayumov, I. V. Rabinov, V. I. Richter, Y. S. Skoblov, and P. G. Chistyakov. 1989. Studies of the functional topography of *Escherichia coli* RNA polymerase: a method for localisation of the sites of affinity labelling. *Eur. J. Biochem.* **180**:577–585.
 31. Harrison, S. C. 1984. Multiple modes of subunit association in the structure of simple spherical viruses. *Trends Biochem. Sci.* **9**:345–351.
 32. Jayasuriya, A. K., M. L. Nibert, and B. N. Fields. 1988. Complete nucleotide sequence of the M2 gene segment of reovirus type 3 Dearing and analysis of its protein product μ 1. *Virology* **163**:591–602.
 33. Joklik, W. K. 1983. The reovirus particle, p. 9–78. *In* W. K. Joklik (ed.), *The reoviridae*. Plenum Publishing Corp., New York.
 34. Kashlev, M., J. Lee, K. Zalenskaya, V. Nikiforov, and A. Goldfarb. 1990. Blocking of the initiation-to-elongation transition by a transdominant RNA polymerase mutation. *Science* **248**:1006–1009.
 35. Kozak, M. 1981. Possible role of flanking nucleotides in recognition of the AUG initiator codon by eukaryotic ribosomes. *Nucleic Acids Res.* **9**:5233–5252.
 36. Kyte, J., and R. F. Doolittle. 1982. A simple method for displaying the hydrophobic character of a protein. *J. Mol. Biol.* **157**:105–132.
 37. Laemmli, U. K. 1970. Cleavage of structural proteins during the assembly of the head of bacteriophage T4. *Nature (London)* **227**:680–685.
 38. Lamb, R. A. 1983. The influenza virus RNA segments and their encoded proteins, p. 21–69. *In* P. Palese and D. W. Kingsbury (ed.), *Genetics of influenza viruses*. Springer-Verlag, New York.
 39. Landon, M. 1977. Cleavage of aspartyl-prolyl bonds. *Methods Enzymol.* **47**:145–149.
 40. Leszczynski, J. F., and G. D. Rose. 1986. Loops in globular proteins: a novel category of secondary structure. *Science* **234**:849–855.
 41. Mallon, R. G., D. Wojciechowicz, and V. Defendi. 1987. DNA-binding activity of papillomavirus proteins. *J. Virol.* **61**:1655–1670.
 42. McCrae, M. A., and W. K. Joklik. 1978. The nature of the polypeptide encoded by each of the ten double-stranded RNA segments of reovirus type 3. *Virology* **89**:578–593.
 43. Mitchell, D. B., and G. W. Both. 1990. Completion of the genomic sequence of the simian rotavirus SA11: nucleotide sequences of segments 1, 2, and 3. *Virology* **177**:324–331.
 44. Morozov, S. Y. 1989. A possible relationship of reovirus putative RNA polymerase to polymerases of positive-strand RNA viruses. *Nucleic Acids Res.* **17**:5394.
 45. Munemitsu, S. M., J. A. Atwater, and C. E. Samuel. 1986. Biosynthesis of reovirus-specified polypeptides: molecular cDNA cloning and nucleotide sequence of the reovirus serotype 1 Lang strain bicistronic S1 mRNA which encodes the minor capsid polypeptide σ 1a and the nonstructural polypeptide σ 1bns. *Biochem. Biophys. Res. Commun.* **140**:508–514.
 46. Mustoe, T. A., R. F. Ramig, A. H. Sharpe, and B. N. Fields. 1978. Genetics of reovirus: identification of the dsRNA segments encoding the polypeptides of the μ and σ size classes. *Virology* **89**:594–604.
 47. Nagata, L., S. A. Masri, and D. C. Mah. 1984. Molecular cloning and sequencing of the reovirus (serotype 3) S1 gene which encodes the viral cell attachment protein sigma 1. *Nucleic Acids Res.* **12**:8699–8710.
 48. Nibert, M. L. Unpublished observation.
 49. Nibert, M. L., T. S. Dermody, and B. N. Fields. 1990. Structure of the reovirus cell-attachment protein: a model for the domain organization of σ 1. *J. Virol.* **64**:2976–2989.
 50. Ovchinnikov, Y. A., G. S. Monastyrskaya, V. V. Gubanov, S. O. Guryev, O. Y. Chertov, N. N. Modyanov, U. A. Grinkevich, I. A. Makarova, T. V. Marchenko, I. N. Prolovnikova, V. M. Lipkin, and E. D. Sverdlov. 1981. The primary structure of *Escherichia coli* RNA polymerase. Nucleotide sequence of the *rpoB* gene and amino acid sequence of the β subunit. *Eur. J. Biochem.* **116**:621–629.
 51. Pabo, C. O., and R. T. Sauer. 1984. Protein-DNA recognition. *Annu. Rev. Biochem.* **53**:293–321.
 52. Pearson, W. R., and D. L. Lipman. 1988. Improved tools for biological sequence comparison. *Proc. Natl. Acad. Sci. USA* **85**:2444–2448.
 53. Ptashne, M. 1988. How eukaryotic transcriptional activators work. *Nature (London)* **335**:683–689.
 54. Ralph, S. J., J. D. Harvey, and A. R. Bellamy. 1980. Subunit structure of the reovirus spike. *J. Virol.* **36**:894–896.
 55. Ralph, W. W., T. Webster, and T. F. Smith. 1987. A modified Chou and Fasman protein structure algorithm. *Comput. Appl. Biosci.* **3**:211–216.
 56. Ramig, R. F., R. K. Cross, and B. N. Fields. 1977. Genome RNAs and polypeptides of reovirus serotypes 1, 2, and 3. *J. Virol.* **22**:726–733.
 57. Ramig, R. F., T. A. Mustoe, A. H. Sharpe, and B. N. Fields. 1978. A genetic map of reovirus. II. Assignment of the double-stranded RNA-negative mutant groups C, D, and E genome segments. *Virology* **85**:531–534.
 58. Richardson, M. A., and Y. Furuichi. 1983. Nucleotide sequence of reovirus genome segment S3 encoding nonstructural protein sigma NS. *Nucleic Acids Res.* **11**:6399–6408.
 59. Samuel, C. E. 1983. Biosynthesis of reovirus-specified peptides, p. 219–230. *In* R. W. Compans and D. H. L. Bishop (ed.), *Double-stranded RNA viruses*. Elsevier Biomedical, New York.
 60. Schiff, L. A., M. L. Nibert, M. S. Co, E. G. Brown, and B. N. Fields. 1988. Distinct binding sites for zinc and double-stranded RNA in the reovirus outer capsid protein σ 3. *Mol. Cell. Biol.* **8**:273–283.
 61. Schiffer, M., and A. B. Edmundson. 1967. Use of helical wheels to represent the structures of proteins and to identify segments with helical potential. *Biophys. J.* **7**:121–135.
 62. Seliger, L. S., K. Zheng, and A. J. Shatkin. 1987. Complete nucleotide sequence of reovirus L2 gene and deduced amino acid sequence of viral mRNA guanylyltransferase. *J. Biol. Chem.* **262**:16289–16293.
 63. Smith, R. E., H. J. Zweerink, and W. K. Joklik. 1969. Polypeptide components of virions, top component and cores of reovirus type 3. *Virology* **39**:791–810.
 64. Smith, R. F., and T. F. Smith. 1990. Automatic generation of primary sequence patterns from sets of related protein sequences. *Proc. Natl. Acad. Sci. USA* **87**:118–122.
 65. Tarlow, O., J. G. McCorquodale, and M. A. McCrae. 1988. Molecular cloning and sequencing of the gene M2 encoding the major virion structural protein μ 1- μ 1C of serotypes 1 and 3 of mammalian reoviruses. *Virology* **164**:141–146.
 66. Towbin, H., T. Staehelin, and J. Gordon. 1979. Electrophoretic transfer of proteins from polyacrylamide gels to nitrocellulose sheets: procedure and some applications. *Proc. Natl. Acad. Sci. USA* **79**:4350–4354.
 67. Tsao, J., M. S. Chapman, M. Agbandje, W. Keller, K. Smith, H. Wu, M. Luo, T. J. Smith, M. G. Rossman, R. W. Compans, and C. R. Parrish. 1991. The three-dimensional structure of canine

- parvovirus and its functional implications. *Science* **251**:1455–1463.
68. **White, C. K., and H. J. Zweerink.** 1976. Studies on the structure of reovirus cores: selective removal of polypeptide λ 2. *Virology* **70**:171–180.
 69. **Wiener, J. R., J. A. Bartlett, and W. K. Joklik.** 1989. The sequences of reovirus serotype 3 genome segments M1 and M3 encoding the minor protein μ 2 and the major nonstructural protein μ ns, respectively. *Virology* **169**:293–304.
 70. **Wiener, J. R., and W. K. Joklik.** 1987. Comparison of the reovirus type 1, 2, and 3 S3 genome segments encoding the nonstructural protein sigma NS. *Virology* **161**:332–339.
 71. **Wiener, J. R., and W. K. Joklik.** 1988. Evolution of reovirus genes: a comparison of serotype 1, 2, and 3 M2 genome segments which encode the major structural capsid protein μ 1C. *Virology* **163**:603–613.
 72. **Wiener, J. R., and W. K. Joklik.** 1989. The sequences of the reovirus serotype 1, 2, and 3 L1 genome segments and analysis of the mode of divergence of the reovirus serotypes. *Virology* **169**:194–203.
 73. **Wiener, J. R., T. McLaughlin, and W. K. Joklik.** 1989. The sequences of the S2 genome segments of reovirus serotype 3 and of the dsRNA-negative mutant ts447. *Virology* **170**:340–341.